AD-A159 431 REDOX CAPACITY ANN DC ELECTRON CONDUCTIVITY IN ELECTROACTIVE MATERIALS(U) NORTH CAROLINA UNIV AT CHAPEL HILL DEPT OF CHEMISTRY R W MURRAY SEP 85 TR-15 1/1

UNCLASSIFIED N00014-82-K-0337 FFG 11/9 NL

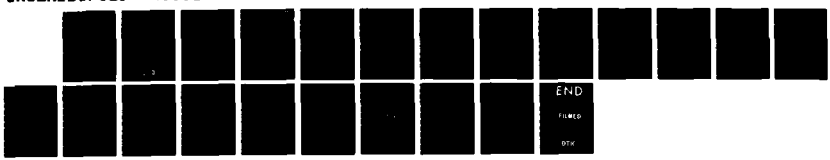

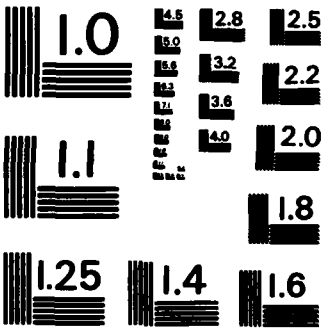

(2)

OFFICE OF NAVAL RESEARCH

Contract N00014-82-K-0337

TECHNICAL REPORT # 15

Redox Capacity and DC Electron Conductivity in Electroactive Materials

by

Royce W. Murray, Principal Investigator

Department of Chemistry

University of North Carolina

Chapel Hill, North Carolina 27514

Prepared for publication in the Journal of Physical Chemistry

1. REPORT NUMBER: Technical Report #15	2. GOVT ACCESSION NO.: AD-A159431
3. RECIPIENT'S CATALOG NUMBER	
4. TITLE (and Subtitle): Redox Capacity and DC Electron Conductivity in Electroactive Materials	5. TYPE OF REPORT & PERIOD COVERED
	6. PERFORMING ORG. REPORT NUMBER
7. AUTHOR(s): Christopher E. D. Chidsey and Royce W. Murray	8. CONTRACT OR GRANT NUMBER(s)
9. PERFORMING ORGANIZATION NAME AND ADDRESS: Department of Chemistry, University of North Carolina, Chapel Hill, NC 27514	10. PROGRAM ELEMENT, PROJECT, TASK AREA & WORK UNIT NUMBERS
11. CONTROLLING OFFICE NAME AND ADDRESS: Office of Naval Research, Department of the Navy, Arlington, Virginia 22217	12. REPORT DATE: SEPT. 85
	13. NUMBER OF PAGES
14. MONITORING AGENCY NAME & ADDRESS (if different from Controlling Office)	15. SECURITY CLASS. (of this report): Unclassified
	15a. DECLASSIFICATION/DOWNGRADING SCHEDULE

16. DISTRIBUTION STATEMENT (of this Report)

Approved for Public Release, Distribution Unlimited

17. DISTRIBUTION STATEMENT (of the abstract entered in Block 20, if different from Report)

18. SUPPLEMENTARY NOTES

19. KEY WORDS (Continue on reverse side if necessary and identify by block number)

redox capacity, electron conductivity, macroscopic quantities, microscopic variations

Sigma Subscript e (rho)

20. ABSTRACT (Continue on reverse side if necessary and identify by block number)

The storage and transport of charge in electroactive materials are closely related. We develop the macroscopic concepts of redox capacity, ρ, and DC electronic conductivity, σ_e. Their ratio, $D_e = \sigma_e/\rho$, is identified as the electron diffusion coefficient. A microscopic model is developed incorporating interaction among the stored electrons and variation of counterion activity as a function of electrochemical potential. Data obtained for the polymer poly[Os(2,2'-bipyridine)$_3$(4-vinylpyridine)$_2$]$^{2+}$(ClO$_4^-$)$_x$ (x = 0-3) are compared with the model. The dependence of the electron diffusion coefficient on electrochemical potential is particularly revealing of discrepancies between the real material and the model, suggesting that this quantity will be useful parameter for the characterization of a variety of electroactive materials.

DD FORM 1 JAN 73 1473 EDITION OF NOV 65 IS OBSOLETE

SECURITY CLASSIFICATION OF THIS PAGE (When Data Entered)

Redox Capacity and DC Electron Conductivity in Electroactive Materials

Christopher E. D. Chidsey

AT&T Bell Laboratories
Murray Hill, New Jersey 07974

Royce W. Murray

Department of Chemistry
University of North Carolina
Chapel Hill, North Carolina 27510

ABSTRACT

The storage and transport of charge in electroactive materials are closely related. We develop the macroscopic concepts of "redox capacity," ρ, and "DC electron conductivity," σ_e. Their ratio, $D_e = \sigma_e/\rho$, is identified as the electron diffusion coefficient. A microscopic model is developed incorporating interaction among the stored electrons and variation of counterion activity as a function of electrochemical potential. Data obtained for the polymer poly[Os(2,2'-bipyridine)$_3$(4-vinylpyridine)$_2$] $(ClO_4)_x$ ($x = 0$–3) are compared with the model. The dependence of the electron diffusion coefficient on electrochemical potential is particularly revealing of discrepancies between the real material and the model, suggesting that this quantity will be a useful parameter for the characterization of a variety of electroactive materials.

Redox Capacity and DC Electron Conductivity in Electroactive Materials

Christopher E. D. Chidsey

AT&T Bell Laboratories
Murray Hill, New Jersey 07974

Royce W. Murray

Department of Chemistry
University of North Carolina
Chapel Hill, North Carolina 27510

Introduction

Electroactive materials have received considerable attention over the last decade both because of curiosity about their basic electrical properties and because of a variety of potential applications. Electroactive materials, in the context of this paper, are solids which exhibit both ion and electron conduction and whose composition can be varied over a wide range by either electrolysis or chemical reaction – often called "doping." These materials include inorganic lattice compounds such as Prussian Blue, $K_xFe_2(CN)_6$ ($x = 0$–2) [1a,b], and lithium-insertion compounds like $Li_xNb_2O_5$ ($x = 0$-1.9) [2a] and $Li_xMo_6Se_6$ ($X = 0$–4) [2b,c]. They also include organic-based polymers ranging from good electron conductors like polypyrrole, $[C_4H_2N(ClO_4)_{.x}]_n$ ($x = 0$-0.4) [3], to relatively poor electron conductors like poly(vinylferrocene), $[(CH_2CHC_5H_4)(C_5H_5)Fe(ClO_4)_{.x}]_n$ ($x = 0$-1) [4a,b].

To electrochemists, at least three features of these materials are of particular significance. The first is their ability to store charge, which we will call redox capacity. The second is their DC electron conduction, and the third is their DC ion conduction. The latter two properties must both be present if charge is to be

stored in the bulk of these materials and not just at their surfaces. The redox capacity and the conductivities are *macroscopic* quantities and are features of all electroactive materials even though there are wide *microscopic* variations among different materials.

Unlike materials in which only ions or only electrons are mobile, electroactive materials generally show a *compositional* gradient at steady state in the presence of an applied bias of either electrons or ions. This feature makes the macroscopic treatment of conduction a little more complex than it is in a single carrier conductor like a metal or an electrolyte solution. Consider for example, making an electron-conduction measurement with chemically inert, metallic electrodes sandwiching a film of the electroactive material. Initially, on application of a potential bias between the electrodes, an electric field exists in the bulk of the material, and electrons flow in response. However, the ions also move in response to that field, and charge develops at the interfaces of the material with the electrodes. This polarization causes the field to decrease in the bulk and increase at the electrode interfaces. Coincident with this decrease of the field, the sample begins to have a compositional gradient with the electroactive material becoming more reduced at the negative electrode and more oxidized at the positive electrode. Now electron motion is driven by the concentration gradient of reduced material (i.e. of electrons) as well as by any residual field.

One major focus of this paper will be the development of an appropriate formalism for describing DC electron conduction. A second major focus will be

the development of a specific microscopic model appropriate for certain electroactive materials and its relation to the general macroscopic formalism. This model incorporates in a simple way two important aspects of real electroactive materials – the dependence of counterion activity on composition and the non-ideal dependence of the electron activity on composition. After developing the model, experimental data for the polymer, poly[$Os(bpy)_2(vpy)_2](ClO_4)_x$ ($x = 0$-3) (bpy = 2,2'-bipyridine, vpy = 4-vinylpyridine) [5] will be examined in the context of both the formalism and the model. At the end, we will briefly discuss ion conduction.

Redox Capacity

One of the important equilibrium properties of an electroactive material is its ability to store charge. This property can be most easily characterized by what we will call in this paper the redox capacity, $\rho(E_{eq})$ (coul V^{-1} cm^{-3} = Fcm^{-3}). It is the charge stored at equilibrium per unit volume per infinitesimal change of the potential across a certain cell. The cell consists of a chemically inert, metallic electrode (eg. Pt) in contact with the electroactive material, an electrolyte and a reference electrode. For experimental ease and accuracy, a counter electrode [6] would generally be used as well so that no charge need be stored in the reference electrode. Mathematically, $\rho(E_{eq})$ is:

$$\rho(E_{eq}) = \frac{dq}{dE_{eq}} = e^2 \frac{dn_e}{d\mu_{ei}} \qquad (1)$$

where q is the charge stored per unit volume, E_{eq} is the equilibrium cell potential, e

is the electron charge, n_e is the number concentration of electrons in the electroactive material and μ_{ei} is the chemical potential of the electron and the added (depleted) amount of cation (anion) needed for electroneutrality [7]:

$$\mu_{ei} = \mu_e + \frac{1}{z_i}\mu_i \tag{2}$$

where μ_e, μ_i and z_i are respectively the electrochemical potential of the electron, the electrochemical potential of the counterion and the charge number of the counterion (positive for cations, negative for anions).

The redox capacity can be obtained from the current observed in a linear sweep voltammogram if charge is stored reversibly in the electroactive material:

$$i = \rho(E_{eq})\, V\, v \tag{3}$$

where V is the volume of the electroactive material and v is the scan rate of the cell potential ($V\ s^{-1}$).

In the presence of a large excess of supporting electrolyte within the electroactive material (not an attainable condition for most materials), the electrochemical potential of the counterion will be constant as the redox state is changed. In that case the redox capacity is:

$$\rho(E_{eq}) = e^2 \frac{dn_e}{d\mu_e} \tag{4}$$

If the electrons all go into equivalent sites and do not interact, then:

$$E_{eq} = E^\circ - (kT/e)\ \ln[\chi_e/(1-\chi_e)] \tag{5}$$

and

$$\rho(E_{eq}) = (n_s e^2/kT)\chi_e(1-\chi_e) \tag{6}$$

where χ_e is the fraction of sites occupied by electrons, k is the Boltzmann constant, T is the absolute temperature, n_s is the number concentration of sites and E° is the standard potential of the sites. These expressions for E_{eq} and $\rho(E_{eq})$ are equivalent to the standard expressions for Nernstian electrochemistry of a surface immobilized species [6]. This relation between redox capacity and E_{eq} has a full width at half maximum of 90 mV at room temperature. In a later section, a somewhat more realistic model for electroactive materials is examined in which, one, the counterion concentration is not assumed to be constant as the redox state is changed and two, the electrons do interact.

DC Electron Conductivity

The conventional definition of conductivity is the ratio of the current density to electric field. The electric field in a "conventional" electronic conductor (eg. a metal) is normally determined from the potential difference between two metal probes divided by the probe separation. However, in an electroactive material (assuming the probe-electroactive material interface passes electrons but not ions), the same measurement determines the gradient of the electron free energy per unit charge, which only has the *units* of an electric field. The potential difference between two probes, ΔE, is just the difference in electron free energy per unit charge between those two points:

$$\Delta E = -(1/e)\Delta\mu_e\ . \tag{7}$$

We show now that the DC electron current density, j_e, is proportional to the gradient of E. The proportionality factor will be called the DC electron conductivity, σ_e, and has units of a current density divided by an electric field ($A\ V^{-1}\ cm^{-1} = ohm^{-1}\ cm^{-1} = Scm^{-1}$). A general approach to charge and mass transport for small perturbations from equilibrium can be based on non-equilibrium thermodynamics [7]. Given that there is a *local* thermodynamic equilibrium so that the local chemical potential μ_ℓ of each species ℓ is defined, the gradient of μ_ℓ is related to the fluxes J_m of species m, by:

$$n_\ell \nabla\mu_\ell = \sum_m K_{\ell m}[(J_m/n_m) - (J_\ell/n_\ell)] \qquad (8)$$

where n_ℓ is the number concentration of species ℓ and the $K_{\ell m}$ are friction or interaction coefficients. Eqn. 8 states that the force exerted on species ℓ per volume element must equal the sum of drag terms proportional to the average velocity of species m relative to species ℓ. At steady state with ion-blocking electrodes, all the fluxes except that of the electrons are zero. The DC current density is:

$$j_e = -eJ_e = -\sigma_e \nabla E \qquad (9)$$

where:

$$\sigma_e = e^2 n_e^2 / (\sum_{m \neq e} K_{em}). \qquad (10)$$

The subscript e designates electrons, and the sum is over all species except the electrons.

The DC electron conductivity depends on the redox state of the material.

Qualitatively, there must be electrons present, *and* there must be unoccupied states for them to move to. This condition is often called mixed-valent [8]. Alternatively, one can say that there must be a large number of different ways of arranging the electrons without significant change of the total energy. Thus it is useful to parameterize conductivities in terms of a transport factor and a statistical factor. In dilute electrolyte solutions, for instance, ionic conductivities are usually parameterized in terms of the ion mobility (a transport factor) and the ion concentration (a statistical factor). However, in electroactive polymers the electron mobility varies with electron concentration for purely statistical reasons; as the available sites fill up with electrons the electron mobility drops. This observation suggests alternative parameterizations of the DC electron conductivity. We will choose to parameterize the DC electron conductivity as a product of a diffusion coefficient and the redox capacity of the material, $\rho(E_{eq})$, discussed in the last section. We will call the diffusion coefficient that results from this choice the electron diffusion coefficient, $D_e(E_{eq})$:

$$D_e(E_{eq}) \equiv \sigma_e(E_{eq})/\rho(E_{eq}). \qquad (11)$$

Since the DC electron conductivity can be measured by applying a small potential gradient, ∇E, to a sample poised at an equilibrium potential, E_{eq}, the experimental electron diffusion coefficient can also be measured at that specific equilibrium potential.

For D_e to be a true diffusion *constant* it would have to be independent of E_{eq}. In the previously mentioned limit of non-interacting electrons with a large excess of

supporting electrolyte, it is independent [9], and Eqn. 9 reduces to Fick's First Law:

$$j = e D_e \nabla n_e \tag{12}$$

where Eqns. 4, 7 and 11 have also been used. This result shows that we have defined D_e in Eqn. 11 in such a way that it is the conventional electron diffusion constant that numerous workers have used to characterize the electron transport in electroactive materials [4a,b;10].

A More Realistic Model

To explore the concepts of redox capacity and DC electron conductivity further, a model will be developed which allows for realistic ion concentrations and, in a simple way, interaction between electrons. Though not particularly novel theoretically, this model does provide an explicit example of a non-Nernstian electroactive material for comparison with experiment. It consists of a simple cubic lattice of oxidized sites each with charge $z_s e$, counterions of charge $z_i e$ and electrons of charge $-e$. The lattice dimension is assumed not to change upon reduction. The number concentration of sites is n_s and the number concentration of electrons is $n_e = n_s \chi_e$ where χ_e is the fraction of sites occupied by electrons. Electrolyte partioning into the electroactive lattice is taken to have a negligible effect on the counterion concentration. This assumption is a reasonable starting point for most electrolyte solutions and most electroactive materials. Nearly non-ionic materials would be an exception. The number concentration, of counterions n_i, is thus:

$$n_i = n_s \chi_i = n_s(\chi_e - z_s)/z_i \tag{13}$$

where χ_i is the number of counterions per site.

Interactions between occupied sites are included in the form of a potential u between those neighboring lattice sites which are both occupied. The number of neighbors to a given site is γ. Each electron is localized by its polarization of its site so that hopping is an activated process requiring the partial depolarization of the occupied site and polarization of the site to be occupied. For simplicity, the counterions are taken to interact with neither each other nor the sites except through an overall electrostatic potential, ϕ, determined by the charge distribution and the applied fields. It is assumed that any space charge which develops represents negligible differences in the concentrations of positively and negatively charged species. This model has been adapted from the theory of "regular solutions" [11] as originally suggested for Prussian Blue by Ellis *et. al.* [1a], and from the mean-field theory of a lattice gas as used for $Li_xMo_6Se_8$ by Coleman *et al.* [2c]. Here we focus on electron-electron interactions though the treatment is the same for ion-ion interactions.

In order to determine the chemical potential of the electrons, we first need to determine their energy on the lattice. Relative to isolated electrons on the lattice at zero potential, the energy of the electrons, U_e, is:

$$U_e = n_{ee} u - n_e e \phi \tag{14}$$

where n_{ee} is the number of pairs of neighboring occupied sites. The partition function for electrons, Q_e, is:

$$Q_e = \sum_{n_{ee}} g(n_e, n_{ee}) \exp(-U_e/kT) \tag{15}$$

where $g(n_e, n_{ee})$ is the number of ways of arranging n_e electrons on a lattice of unit volume such that there are n_{ee} pairs of neighboring sites which are both occupied. The chemical potential of the electrons, μ_e is:

$$\mu_e = -kT\, d(\ell n Q_e)/dn_e \tag{16}$$

If the exponential in the partition function varies little over the range of n_{ee} for which $g(n_e, n_{ee})$ is significant, one can make a mean-field approximation and remove the exponential of the average value of $-U_e/kT$ over n_{ee} from the summation. The resulting summation of $g(n_e, n_{ee})$ over n_{ee} is just the number of ways of arranging n_e identical electrons on n_s sites. After substantial manipulation, one obtains:

$$\mu_e = \epsilon\chi_e - e\phi + kT\, \ell n[\chi_e/(1-\chi_e)] \tag{17}$$

where the occupied site interaction energy, $\epsilon \equiv \gamma u$, has been introduced. The first term in Eqn. 17 is the contribution of the occupied site-occupied site interactions to the electron chemical potential. The second and third terms are respectively the electrostatic and entropic contributions to μ_e. Both these latter terms are present even for $\epsilon = 0$. In the theory of regular solutions, this approximation is often called the zeroth-order [11] or Bragg-Williams approximation [12]. With nearest-neighbor interactions only ($\gamma = 6$ for a simple cubic lattice), it is valid when ϵ is small compared with kT and continues to give a qualitatively appropriate treatment when ϵ is of the order of kT. Beyond that range, occupied site-occupied site interactions cause substantial ordering of the occupation patterns. For instance, for

ϵ large and positive (repulsive) the occupied sites avoid each other and alternating site occupancy is expected leading ultimately to *compound formation*. With u large and negative (attractive) occupied sites group together resulting ultimately in *phase separation*. On the other hand, as pointed out by Coleman *et al.* [2c], the mean-field treatment is exact if each site interacts with many others ($\gamma \to \infty$; $u \to 0$; ϵ finite).

Parameters analogous to the occupied site interaction energy, ϵ, have appeared in numerous treatments of electroactive film voltammetric waveshapes in the past, sometimes invoked as *ad hoc* parameters to modify an ideal activity expression. Ikeda *et. al.* introduced a "G" [13] that is analogous to $-\epsilon/kT$. Laviron [14] has also used a "G" which is analogous to $-\frac{1}{2}\epsilon/kT$. Ellis *et. al.* [1a] define an energy "W_{ab}" which is $-\frac{1}{2}N_A\epsilon$. (N_A is Avogadro's number.) Coleman *et al.* [2c] defined an energy U which is ϵ/γ.

Having obtained the chemical potential of the electrons we now need that of the counterions. These are taken to be noninteracting, charged particles in this model, and thus their chemical potential, μ_i, is:

$$\mu_i = kT \ln\chi_i + z_i e\phi\,. \tag{18}$$

The equilibrium cell potential is:

$$E_{eq} = -(1/e)(\mu_e + \frac{1}{z_i}\mu_i) + \text{constant} \tag{19}$$

$$= -(\epsilon/e)\chi_e - (kT/e)\{\ln[\chi_e/(1-\chi_e)] + (1/z_i)\ln[(\chi_e - z_i)/z_i]\} + \text{constant}\,.$$

The redox capacity is:

$$\rho(E_{eq}) = \frac{dq}{dE_{eq}} = (n_s e^2/kT)[\epsilon/kT + \chi_e^{-1} + (1-\chi_e)^{-1} + z_i^{-1}(\chi_e - z_s)^{-1}]^{-1} \quad (20)$$

In Fig. 1A. $\rho(E_{eq})$ curves are plotted vs. E_{eq} for several values of z_s with $\epsilon = 0$ (no occupied site interaction). The curve labelled $z_s = \infty$ corresponds to the limit of a large excess of supporting electrolyte. Note that in those cases in which the material is ionic at all electron concentrations ($z_s = +3$ and $+2$) the curves are qualitatively quite similar to that limit. In the case of $z_s = +1$ the redox capacity is somewhat unsymmetric with the peak displaced to more positive potentials and with a long tail at negative potentials as the non-ionic reduced form is approached. These features are the result of the counterion activity changing substantially as the chemical composition of the material changes. At 25°C, the full width at half maximum of these curves are 90.7, 102, 109 and 132 mV for $z_s = \infty$, +3, +2 and +1 respectively. Fig. 2A shows the redox capacity curves for various values of ϵ/kT with $z_s = +3$. Note that nearest-neighbor occupied site-occupied site interactions lead to *symmetrical* broadening or narrowing of the capacity curves.

Now consider the DC electron conductivity of this lattice model. Conduction will occur by hopping between a site at position x and the site at x+a where x measures position along the current direction and a is the lattice spacing. The probability, p_f, of a forward hop from x to x+a per site per unit time is:

$$p_f = \chi_e(x)[1 - \chi_e(x+a)]k_f \quad (21)$$

and that of a reverse hop, p_r, is:

$$p_r = \chi_e(x+a)[1 - \chi_e(x)]k_r \quad (22)$$

where in accord with the mean-field approximation the occupancies of neighboring sites are taken to be uncorrelated. The forward and reverse hop rates, k_f and k_r respectively, are related by a Boltzmann factor:

$$k_f/k_r = \exp\{-[U(x+a) - U(x)]/kT\} \quad (23)$$

where U(x) is the energy of a state with an electron at x and *depends* on the occupancy of neighboring sites.

The electron current density, j_e, is:

$$j_e = -a n_s e \langle p_f - p_r \rangle \quad (24)$$

where $\langle\ \rangle$ denotes the average value. Using Eqn. 23 to eliminate k_f, expanding the exponential to first order and expanding U(x) and $\chi_e(x)$ about x:

$$j_e = (a^2 k_o)(n_s e)[(d\chi_e/dx) + \chi_e(1-\chi_e)\langle dU(x)/dx\rangle/kT] \quad (25)$$

where only the lowest order terms in a have been saved and k_r has been replaced by k_o, the hopping rate in the absence of an energy difference; k_o is negligibly different from k_r. Note that the first term of Eqn. 25 is Fick's First law and that the second term is a correction due to the energetics of the problem. The average energy change per unit displacement of the electron, $\langle dU(x)/dx\rangle$, depends on the electrostatic potential and the probability of having neighboring sites occupied:

$$\langle dU(x)/dx\rangle = \epsilon(d\chi_e/dx) - e(d\phi/dx) \quad (26)$$

From Eqns. 7, 9, 17, 25 and 26 one obtains:

$$j_e = -\sigma_e(E_{eq})(dE/dx) \quad (27)$$

with

$$\sigma_e(E_{eq}) = (a^2k_o)(n_e e^2/kT)\chi_e(1-\chi_e) \quad (28)$$

From Eqns. 11 and 20, the electron diffusion coefficient for this model is:

$$D_e(E_{eq}) = (a^2k_o)\{1 + [z_i^{-1}(\chi_e - z_s)^{-1} + (\epsilon/kT)]\chi_e(1-\chi_e)\} \quad (29)$$

Note that, as mentioned earlier, in the limit of non-interacting sites ($\epsilon = 0$) and a large excess of supporting electrolyte ($z_s = \infty$), $D_e(E_{eq}) = a^2k_o$ and is a diffusion *constant*.

In general $D_e(E_{eq})$ is not constant as the composition of the material is changed, but the changes are not large. Figs. 1B and 2B show D_e values for various values of z_s and ϵ. Note in Fig. 1B that $D_e(E_{eq})$ differs from (a^2k_o) by less than a factor of two even as the fully reduced, non-ionic form of the $z_s = +1$ lattice is approached. Elsewhere and for other values of z_s, much smaller variations are noted. This *relative* constancy of $D_e(E_{eq})$ should be contrasted with the behavior of the electron mobility which as mentioned earlier goes to zero as the lattice is reduced. Within the context of the *present* model the constant, a^2k_o, would clearly be the most appropriate transport factor to choose. However to obtain this value experimentally would require measuring $\chi_e(1-\chi_e)$, a difficult quantity to measure accurately over the full potential range. Furthermore, and more fundamentally, such an approach would *presuppose* the microscopic model appropriate for a given, real, electroactive material. As experimentalists we therefore favor collecting the experimental diffusion coefficient, $D_e(E_{eq})$, as a function of the equilibrium cell potential, E_{eq}. Each value can be obtained from a measurement of $\sigma_e(E_{eq})$ and $\rho(E_{eq})$ with only arbitrarily small potential excursions about each value of E_{eq}.

Microscopic interpretation of $D_e(E_{eq})$ will clearly be model dependent.

Experiments with Poly $[Os(bpy)_2(vpy)_2](ClO_4)_x$ Films

To illustrate the approach to electroactive materials developed here, we now present experimental results for films of the electroactive polymer poly$[Os(bpy)_2(vpy)_2](ClO_4)_x$ (bpy = 2, 2'-bipyridine; vpy = 4-vinylpyridine). This and related materials have been extensively studied in this laboratory [5] and thus provide a logical first target for the application of this new approach. Fig. 3A shows the film capacitance, C, and redox capacity, ρ, from $E_{eq} = +1$ to -2V vs. SSCE (sodium chloride-saturated calomel electrode). In this range the metal-centered reduction of Os(III) to Os(II) is seen at +0.73V, and reduction of first one and then both bipyridine ligands are seen at -1.32V and -1.53V respectively. The states resulting from these two reductions are labelled Os(I) and Os(0) respectively.

The polymer film was deposited on a Pt electrode by reductive electropolymerization of a solution of 0.5 m*M* $Os(bpy)_2(vpy)_2(ClO_4)_2$ and 0.1*M* tetraethylammonium perchlorate (Et_4NClO_4) in acetonitrile (CH_3CN). An overcoat of porous Au was deposited by evaporation [5] and served as a second electrode for electron conduction measurements. Such an assembly is labeled a "sandwich electrode" [15]. For the experiment in Fig. 3A the potential of the Au electrode was not controlled; it was floating. Those data were obtained by linear sweep voltammetry of the Pt electrode with the sandwich immersed in 0.1*M* Et_4NClO_4/CH_3CN. In order to suppress irreversible and interfering processes the

data were taken by sweeping the potential negatively from +1.05V to 0V and by sweeping the potential positively from −2.0 to 0V with correction of sloping baselines by subtraction. With this corrected current, $i_c(E_{eq})$, the film capacitance, $C(E_{eq})$, was taken to be:

$$C(E_{eq}) = i_c(E_{eq})/v \tag{30}$$

where v is the scan rate in (V s^{-1}).

The redox capacity, $\rho(E_{eq})$, is:

$$\rho(E_{eq}) = C(E_{eq})/V \tag{31}$$

where the polymer volume, V, is obtained from the integral of $C(E_{eq})$ across one mixed-valent state (eg. Os(III/II)):

$$V = \int_{Os(II)}^{Os(III)} C(E_{eq})\, dE/(en_s) \; . \tag{32}$$

n_s, the number concentration of sites, is (1.5*M*) N_A [5] where N_A is Avogadro's number. The redox capacity can be read from the right-hand axis in Fig. 3A.

Fig. 3B shows the conductance, $G(E_{eq})$, of the sandwich electrode in 0.1*M* Et_4NClO_4/CH_3CN, obtained by measuring the steady-state current, $i_{ss}(E_{eq})$, flowing with a small bias, ΔE, between the Pt and porous Au electrodes:

$$G(E_{eq}) = i_{ss}(E_{eq})/\Delta E \tag{33}$$

as a function of the potential of the Pt electrode relative to SSCE. The DC electron conductivity, $\sigma_e(E_{eq})$, is:

$$\sigma_e(E_{eq}) = Gd/A = GV/A^2 \tag{34}$$

where d is the thickness of the film, A is the area and V, the volume, is obtained

from Eqn. 32. The DC electron conductivity can be read from the right-hand axis in Fig. 3B.

For each feature in the redox capacity there is a corresponding feature in the DC electron conductivity. However the three conductivity features vary greatly in height whereas the three capacity peaks are all roughly the same. The experimental electron diffusion coefficient, $D_e = \sigma_e/\rho$, is noted for each of the three capacity peaks. The electrons responsible for conduction in the Os(I/0) mixed-valent material are about twenty times more mobile than those in the Os(III/II) mixed-valent material. Put in different terms, the electron self-exchange rate between Os(0) and Os(I) is much larger than that between Os(II) and Os(III) in this material. However, the Os(I) and Os(0) states are not very stable [5]. To examine the dependence of D_e on potential across a redox capacity feature, we looked carefully at the Os(III/II) mixed-valent material.

Linear sweep voltammetry as a technique for determining $\rho(E_{eq})$ suffers considerably from interference by electrochemically irreversible processes. These slow processes can even be intrinsic to the electroactive material in which there may be regions or particular chemical species which only slowly exchange electrons with the bulk of sites. In addition, slow or fast but chemically irreversible redox processes may occur at the metal electrode or in the electrolyte solution. Any of these phenomena will lead to a difference in the absolute magnitude of the current for positive-going versus negative-going linear voltammetric sweeps. One possible solution is to use an AC technique to measure only those processes which are

reversible on a chosen timescale.

Fig. 4A shows the 50 Hz capacitance of a very thin poly[$Os(bpy)_2(vpy)_2$]$(ClO_4)_2$ film on Pt from +1.0 to +0.4V in 1.0*M* Et_4NClO_4/CH_3CN. This data was obtained from the out-of-phase current, i^{out}_{rms}, caused by a small, sinusoidal modulation of the electrode potential (ΔE_{rms} = 2 mV) at $\omega/2\pi$ = 50 Hz:

$$C(E_{eq}) = i^{out}_{rms}/(\Delta E_{rms}\omega) \; . \tag{35}$$

The in-phase current had roughly the same dependence on E_{eq} as i^{out}_{rms} but was less than 5% its magnitude at the maximum and thus negligible in the determination of $C(E_{eq})$. Such a small in-phase current shows that, for this film, electron and ion conduction through the film are fast compared with the 200 ms modulation period. Clearly use of higher frequencies or thicker films could allow measurement of the kinetics of redox charging. In practice thicker films would be required because at this thickness the solution resistance dominated the in-phase current even though a 1 mm reference electrode-to-polymer spacing and a 1.0*M* electrolyte solution were used.

The small, constant background in $C(E_{eq})$ is presumably due to reversible double layer charging and is much smaller than that in the linear sweep voltammetry The small hysteresis for positive-going versus negative-going potential sweeps is due to the finite sweep rate of 0.5 mV/s. Small changes in the 50 Hz capacitance take place for several seconds after an abrupt potential step from one side or the other of the Os(III/II) peak onto the peak. The final value of $C(E_{eq})$ is however

independent of the starting potential. Such small, slow changes may be due to slow structural relaxation in the polymer film.

Fig. 4B shows an expansion of the Os(III/II) conductance and DC electron conductivity data from Fig. 3B. The raw conductance data cannot be compared with the raw capacitance data in Fig. 4A. On the other hand, the DC electron conductivity, σ_e, read from the right-hand axis in Fig. 4B can be compared with the redox capacity, ρ, read from the right-hand axis in Fig. 4A. Their ratio, the experimental electron diffusion coefficient, D_e, (Eqn. 11) is plotted in Fig. 4C. For this calculation the average values of the positive-going and negative-going scans were used. The diffusion coefficient across the central portion of the Os(III/II) wave is about 6×10^{-9} cm^2/s, in good agreement with results obtained with sandwich electrodes under limiting current, large bias conditions [5]. However, the diffusion coefficient decreases substantially at either edge of the Os(III/II) feature, indicating a heterogenity of sites and the presence of more poorly conductive sites with $E_{½}$ values both greater and less than the majority of the sites. Careful examination of the redox capacity (Fig. 3A) indeed reveals a shoulder on the positive potential side of the Os(III/II) feature and a small plateau to negative potentials.

Despite these extra features, it is interesting to compare the curves in Fig. 4 with the model described in the last section. The points in Fig. 4 are calculated from that model with ϵ/e = +13 mV, z_s = +3, z_i = −1 and with the values of n_t and (a^2k_o) in Eqns. 20, 28 and 29 adjusted to fit the maximum values of the

experimental capacity and conductivity. The value of ϵ was chosen to match the full width at half maximum of the observed capacity. The discrepancies between the data and the model are small in Fig. 4A and 4B and are clearly accenuated in the D_e plot in Fig. 4C. The enhancement seen in Fig. 4C suggests that the formalism presented in this paper may have its most powerful use in the careful qualitative analysis of the electron transport properties of real electroactive materials.

Other Electroactive Materials

The model developed above offers a reasonable starting point for discussing the properties of electroactive materials with weakly interacting electron sites and a continuum of counterion sites. In general however, there may be a large dispersion in the energies of electron sites; there may be a finite concentration of counterion sites; there may be a dispersion in the energies of counterion sites; finally, the electron and counterions may interact directly – coupling the motion of electrons and ions. In all cases, the basic macroscopic formalism will still apply.

A dispersion in the energies of electron sites can be the consequence of chemical heterogeneity of the sites, or it may arise due to delocalization as in a metal or semiconductor. Polypyrrole is possibly an example of a material with both chemically heterogeneous and delocalized electron sites [3c, 16]. A dispersion of electron energies could be incorporated into the model developed here by adopting a density of electron energies instead of assuming all states to be of the same energy.

A finite concentration of counterion sites and even a dispersion of ion site energies would be relatively easy to incorporate into the model used here; such features would only change μ_i. However at the point that the availability of ion sites, rather than the availability of electron sites begins to limit the redox capacity, the concept of the "electron diffusion coefficient" as a transport factor begins to change. As an extreme case consider a material with twice as many electron sites as cation sites. Once the cation sites have been filled by reduction, the redox capacity will go to zero, but, because of the presence of unoccupied electron sites, there will still be a finite DC electron conductivity. In this extreme, D_e would be infinite and not a very useful quantity. Clearly this limit borders on the more familiar case of solid state electronic conductors.

In an alternate vein, consider briefly ion conduction. In a material like poly[$Os(bpy)_2(vpy)_2$]$(ClO_4)_x$ with redox conductivity only weakly dependent on the availability of counterion sites, the ion conductivity is not expected to correlate with the redox capacity. On the other hand, certain materials may have redox capacities that are very dependent on the availability of ion sites. That is, electrons can be stored as long as there are energetically accessible sites for the ions. Lithium-insertion compounds such as $Li_xNb_2O_5$ [2a] or $Li_xMo_6Se_8$ [2b] may be examples. In that case the DC ion conductivity would be expected to correlate strongly with the redox capacity. At potentials where the redox capacity was low, there would be few empty ion sites at the same energy as the highest filled sites, and the ion conductivity would be low. At potentials where the redox capacity was high, there would be many empty sites to hop to, and the ion conductivity would be

high. Such materials, if found and characterized, might be very interesting candidates for "ion-gates" [17], which are barriers that potentiostatically control ion flow between two solutions.

Coleman *et al.* [Coleman] have shown that the redox capacity of $Li_xMo_6Se_8$ for $x = 0-1$ is well fit to a mean-field model with an occupied site interaction energy equivalent to $\epsilon/e = -90$ mV in our model. With $Li_xMo_6Se_8$ the redox capacity is thought to be totally dominated by the availability of Li^+ sites. The negative occupied site interaction energy observed is in reasonable agreement with calculations based on the interaction of expansion sites in the lattice due to lithium insertion. In $Li_xMo_6Se_8$ lithium ion conductivities would be expected to correlate with the redox capacity being maximal for $x = 0.5$ over the range $x = 0-1$.

Summary

We have developed a macroscopic formalism to treat charge storage and DC electron conduction in electroactive materials based on the concepts of redox capacity and DC electron conductivity. A transport factor, the electron diffusion coefficient has been proposed and shown to coincide with the diffusion constant defined by Fick's First law when that diffusion law is appropriate. A microscopic model for *some* real electroactive materials has been developed including in simple ways, the effects of both counterion activity and weak electron-electron interaction. Experimental results for poly$[Os(byp)_2(vpy)_2](ClO_4)_x$ have been presented; both a DC and an AC technique for obtaining the redox capacity were explored. We found several small experimental features that were not present in the model but

whose detection was enhanced in a plot of the experimental electron diffusion coefficient. Finally, we have commented briefly on several different types of electroactive materials from the perspective of this formalism, which we believe can provide a unifying macroscopic treatment of this interesting class of materials.

Acknowledgement.

This research was supported in part by the National Science Foundation and the Office of Naval Research.

REFERENCES

1. a. Ellis, D.; Eckhoff, M.; Neff, V. D. *J. Phys. Chem., 1981, 85*, 1225.

   b. Crumbliss, A. L.; Lugg, P. S; Morosoff, N. *Inorg. Chem., 1984, 23*, 4701.

2. a. Cava, R. J.; Murphy, D. W.; Zahurak, S. M. *J. Electrochem. Soc., 1983, 130*, 2345.

   b. Dahn, J. R.; McKinnon, W. R.; Coleman, S. T. *Phys. Rev. B. 1981, 31*, 484.

   c. Coleman, S. T.; McKinnon, W. R.; Dahn, J. R. *Phys. Rev. B. 1984, 29*, 4147.

3. a. Diaz, A. F.; Castillo, J. I. *J. C. S. Chem. Comm., 1980, 1980*, 397.

   b. Pfluger, P.; Krounbi, M.; Street, G. B.; Weiser, G. *J. Chem. Phys., 1983, 78*, 3212.

   c. Feldman, B. J.; Burgmayer, P.; Murray, R. W. *J. Am. Chem. Soc., 1985, 107*, 872.

   d. Kaufman, J. H.; Keiji Kanazawa, K.; Street, G. B. *Phys. Rev. Lett., 1984, 53*, 2461.

4. a. Daum, P.; Lenard, J. R.; Rolison, D. R.; Murray, R. W. *J. Am. Chem. Soc. 1980, 102*, 4649.

   b. Peerce, P. J.; Bard, A. J. *J. Electroanal. Chem., 1980, 114*, 89.

   c. Nowak, R. J.; Schultz, F. A.; Umana, M.; Lam, R.; Murray, R. W. *Anal. Chem., 1980*, 52, 315.

5. Pickup, P. G.; Kutner, W.; Leidner, C. R.; Murray, R. W. *J. Amer. Chem. Soc., 1984, 106* 1991.

6. Bard, A. J.; Faulkner, L. R. *Electrochemical Methods: Fundamentals and Applications*, Wiley: New York, 1980.

7. Newman, J. *Electrochemical Systems*, Prentice-Hall: Englewood Cliffs, New Jersey 1973.

8. Kaufman, F. B.; Schroeder, A. H.; Engler, E. M.; Kramer, S. R.; Chambers, J. Q. *J. Am. Chem. Soc., 1980, 102*, 483.

9. Kutner, R. *Phys. Lett., 1981, 81A*, 239.

10. a. Murray, R. W. *Ann. Rev. Mater. Sci., 1984, 14*, 145.

    b. Andrieux, C. P.; Saveant, M. *J. Electroanal. Chem., 1980, 111*, 377.

    c. Oyama, N.; Anson, F. C. *J. Electrochem. Soc., 1980, 127*, 640.

    d. Laviron, E. *J. Electroanal. Chem., 1980, 112*,, 1.

11. Guggenheim, E. A. *Mixtures - The Theory of the Equilibrium Properties of Some Simple Classes of Mixtures, Solutions and Alloys*, Oxford: London, 1952.

12. Moore, W. J. *Physical Chemistry*, Prentice-Hall: Englewood Cliffs, New Jersey, 1972, p. 273.

13. Ikeda, T.; Leidner, C. R.; Murray, R. W. *J. Electroand. Chem., 1982, 138,* 343.

14. Laviron, E. *J. Electroanal. Chem., 1981, 122,* 37.

15. Chidsey, C. E. D.; Murray, R. W. *Science* submitted.

16. Yakushi, K.; Lauchlan, L. J.; Clarke, T. C.; Street, G. B. *J. Chem. Phys., 1983, 79,* 4774.

17. Burgmayer, P.; Murray, R. W. *J. Phys. Chem., 1984, 88,* 2515.

FIGURE CAPTIONS

Figure 1. A) Redox capacities, ρ, calculated from Eqns. 19 and 20 and B) electron diffusion coefficients, D_e, from Eqn. 29 for various values of z_s with $\epsilon = 0$ and $z_i = -1$.

Figure 2. A) Redox capacities, ρ, calculated from Eqns. 19 and 20 and B) electron diffusion coefficients, D_e, from Eqn. 29 for various values of ϵ/kT with $z_s = +3$ and $z_i = -1$.

Figure 3. A) Film capacitance, C, and redox capacity, ρ, and B) film conductance, G, and DC electron conductivity, σ_e, of a 2.2×10^{-8} mol/cm^2 poly[Os(bpy)$_2$(vpy)$_2$](ClO$_4$)$_2$ film sandwiched between Pt and porous Au electrodes and immersed in 0.1*M* Et_4NClO_4/CH_3CN. Film area $A = 0.0032$ cm^2; film thickness $d = 150$ nm (from volume, V, determined as described in text). C determined from linear sweep voltammetry as described in text. Scan rate $v = 50$ mV/s. G determined with $\Delta E = 20$ mV and $v = 50$ mV/s. Experimental electron diffusion coefficients, D_e, determined at capacity maxima.

Figure 4. A) Film capacitance, C, and redox capacity, ρ, of a very thin 2×10^{-9} mol/cm^2 poly[Os(bpy)$_2$(vpy)$_2$](ClO$_4$)$_2$ film in the Os(III/II) composition range on a Pt electrode and immersed in 1.0*M* Et_4NClO_4/CH_3CN (solid curves). Film area $A = 0.073$ cm^2;

film thickness d = 13 nm (from volume, V, determined as described in text). C determined from out-of-phase current of AC voltammogram as described in text. Scan rate v = 0.5 mV/s; frequency $\omega/2\pi$ = 50 Hz; ΔE_{rms} = 2 mV.

B) Film conductance, G, and DC electron conductivity, σ_e, (solid curves) expanded from Fig. 3B.

C) Experimental electron diffusion coefficient, D_e (solid curve).

Points in all panels are calculated using Eqns. 19, 20, 28 and 29 with $\epsilon/e = -0.5$, $z_s = +3$ and $z_i = -1$.

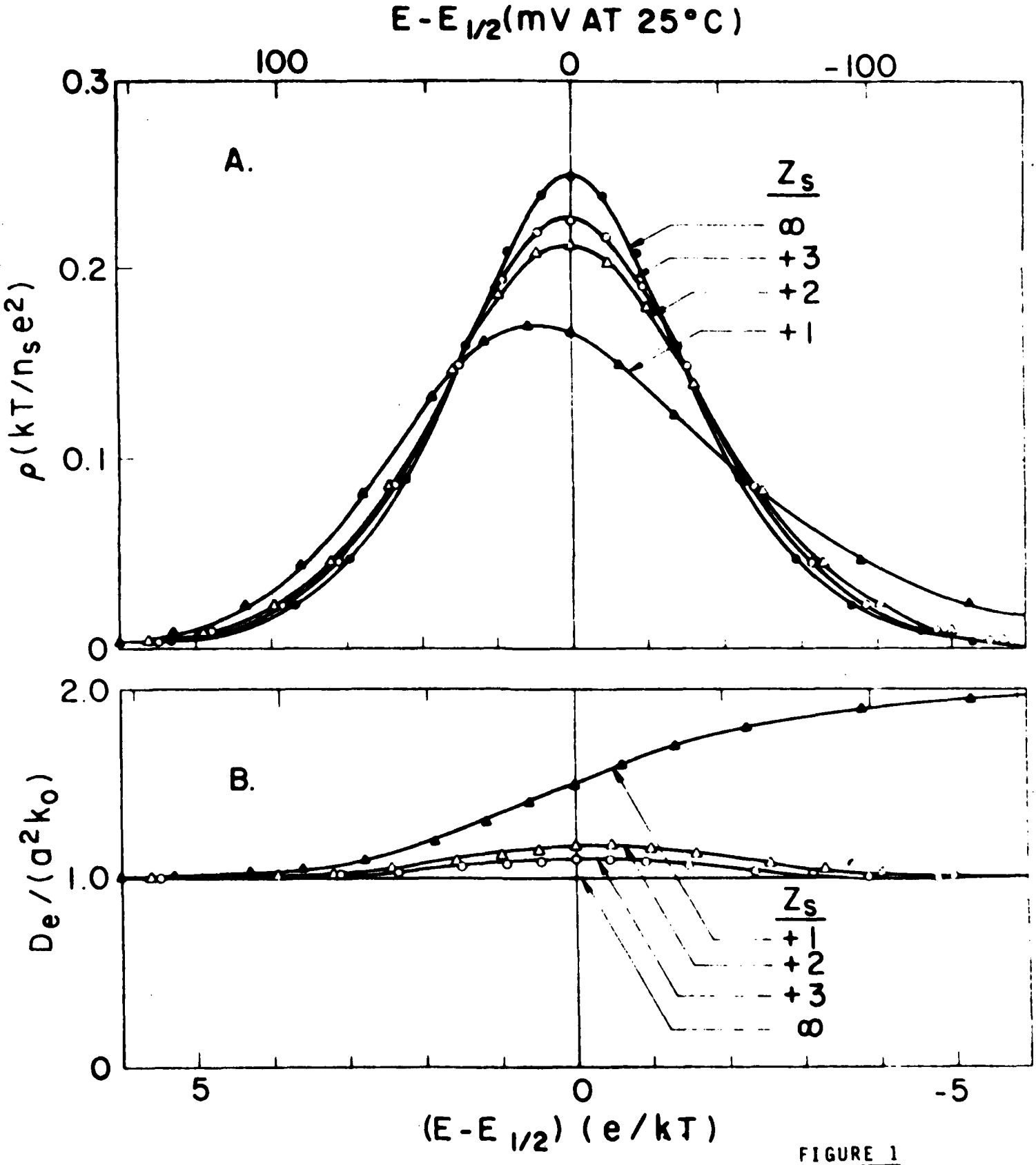

FIGURE 1

C. Chidsey & R. W. Murra

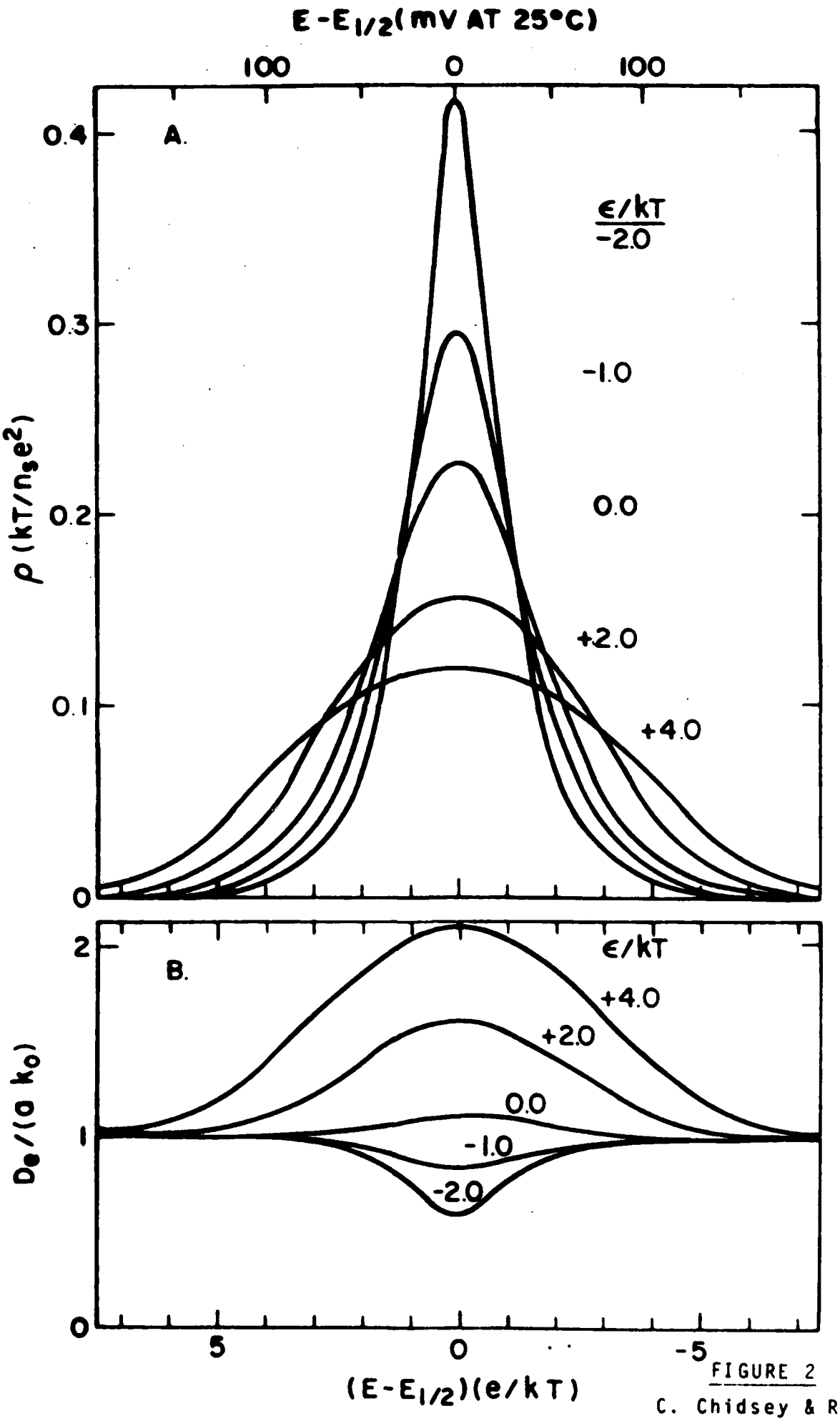

FIGURE 2

C. Chidsey & R.W. Murray

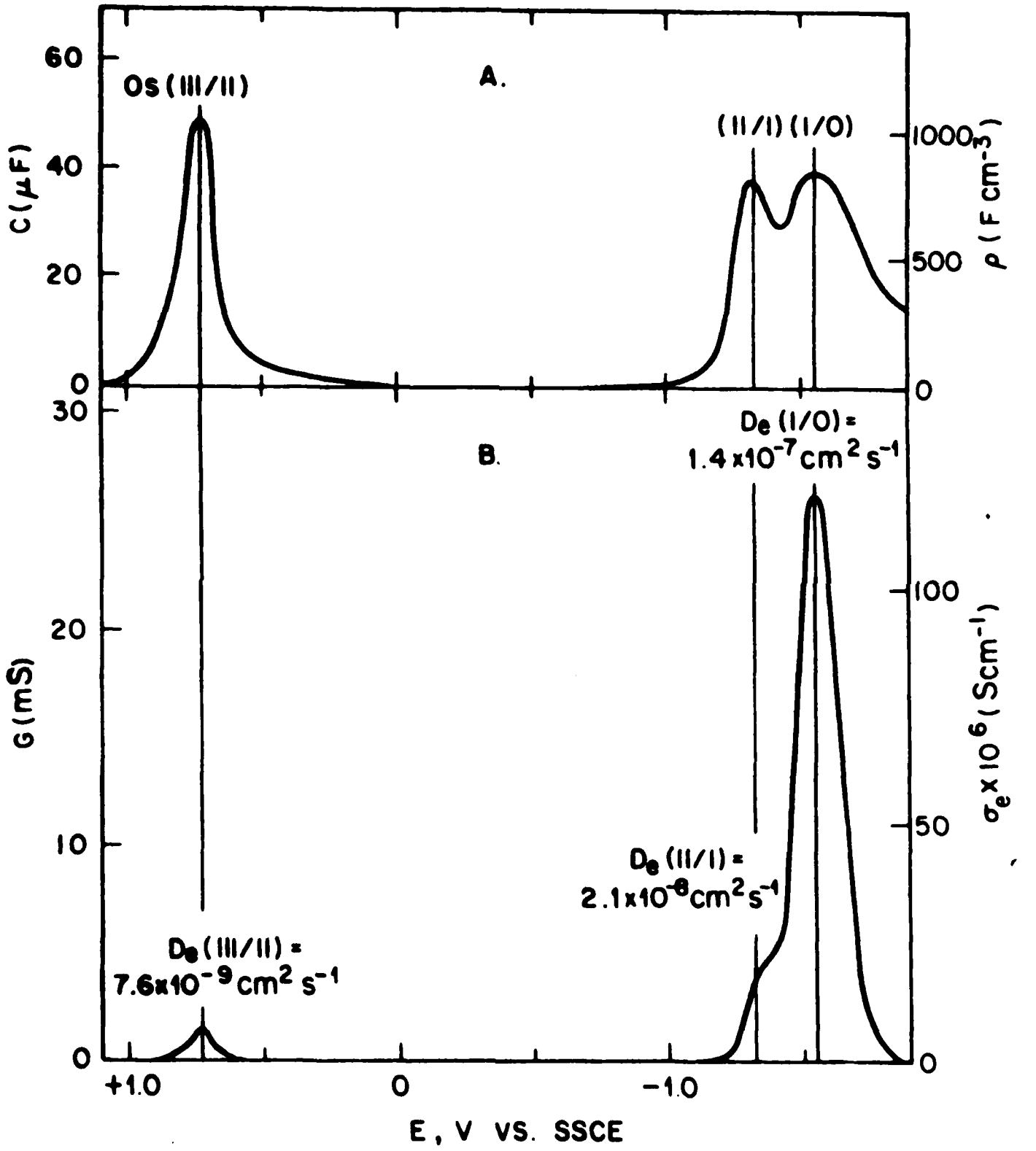

FIGURE 3

C. Chidsey & R. W. Murray

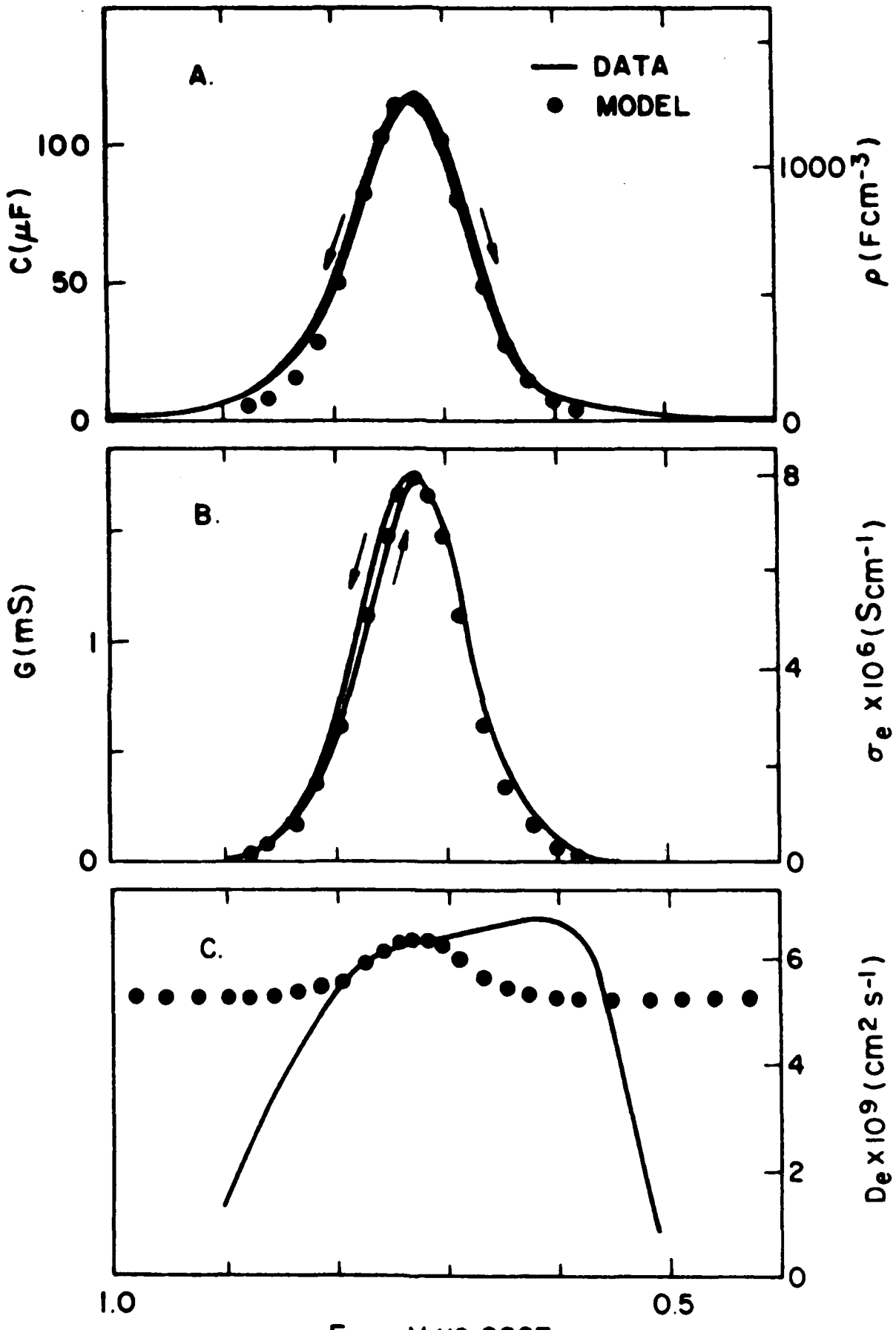

FIGURE 4

C. Chidsey & R. W. Murray

END

FILMED

11-85

DTIC